

Charge transfer, valence, and the metal-insulator transition in $\text{Pr}_{0.5}\text{Ca}_{0.5}\text{CoO}_3$

K. Knížek, J. Hejtmánek, P. Novák, and Z. Jirák

Institute of Physics, ASCR, Cukrovarnická 10, 162 00 Prague 6, Czech Republic

(Received 13 February 2010; published 15 April 2010)

Generalized gradient approximation (GGA) + U electronic-structure calculations evidence that the recently observed simultaneous metal-insulator and spin-state transition in perovskite cobaltite $\text{Pr}_{0.5}\text{Ca}_{0.5}\text{CoO}_3$ is accompanied by a charge transfer between Pr and Co cations from $0.5 \text{Pr}^{3+} + \text{Co}^{3.5+}$ toward $0.5 \text{Pr}^{4+} + \text{Co}^{3+}$. The metal-insulator transition is a result of the interplay between covalency of the Pr-O bond and increasing stability of the insulating low-spin configuration with decreasing valency of Co cation. Our calculations explain why this type of transition is encountered in the Pr-based system only.

DOI: [10.1103/PhysRevB.81.155113](https://doi.org/10.1103/PhysRevB.81.155113)

PACS number(s): 71.30.+h, 71.15.Mb, 75.30.Wx

I. INTRODUCTION

Heavily doped perovskite cobaltites such as $\text{La}_{1-x}\text{Sr}_x\text{CoO}_3$ ($x > 0.2$) are ferromagnetic metals with Fermi level dominated by a hybridized $\text{Co}(3d)\text{-O}(2p)$ band. The cobalt ground state is defined as $t_{2g}^5\sigma^{1-x}$ and the carriers can be viewed as low spin (LS $S=1/2$, t_{2g}^5) Co^{4+} ions moving in the matrix of intermediate spin (IS $S=1$, $t_{2g}^5e_g^1$) Co^{3+} ions. The isovalent substitution of La or Sr by smaller rare-earth or Ca cations results in a decrease in the carrier mobility due to increasing tilt of the CoO_6 octahedra and subsequent decrease in the bandwidth. Finally, a new highly resistive ground state, consisting of a mixture of LS (t_{2g}^6 , $S=0$) Co^{3+} and LS Co^{4+} ions, is stabilized. This compositional transition is encountered in the $\text{Ln}_{1-x}\text{Ca}_x\text{CoO}_3$ system between $\text{Ln} = \text{Nd}$ and Sm .¹ The experiments, performed on $\text{Sm}_{0.7}\text{Ca}_{0.3}\text{CoO}_3$, suggest that the spin state of cobalt only slowly varies with temperature, reflecting a thermal excitation from the diamagnetic LS Co^{3+} to closely lying paramagnetic Co^{3+} states of IS or high spin (HS $S=2$, $t_{2g}^4e_g^2$) character. This reminds the well-known situation in pure or lightly doped LaCoO_3 .²

The present study concerns rather unique case of the praseodymium-based system at $x \sim 0.5$ that deviates from the above-mentioned trend in $\text{Ln}_{1-x}\text{Ca}_x\text{CoO}_3$ with the Ln size.^{3,4} At ambient temperature, the spin states are of the $\text{Co}^{3.5+}$ ($t_{2g}^5\sigma^{0.5}$) character with dominant ferromagnetic (FM) interactions, similar as in the systems based on the larger-size lanthanum or smaller-size neodymium. On cooling, just before the FM ground state is expected to be formed, the $\text{Pr}_{0.5}\text{Ca}_{0.5}\text{CoO}_3$ compound undergoes a simultaneous spin-state and metal-insulator (M-I) transition at 90 K. It is manifested by a pronounced peak of the specific heat, drop of the paramagnetic susceptibility, and volume contraction to about 2%. A similar transition has been later observed on less doped samples $\text{Pr}_{1-x}\text{Ca}_x\text{CoO}_3$ ($x=0.3$) under high pressures or upon a partial substitution of praseodymium by smaller rare-earth cations or yttrium.^{1,5,6} The cobalt states in the low-temperature phase have been interpreted as a mixture of LS Co^{3+} and LS Co^{4+} ions, which seemingly fits the effective paramagnetic moments actually observed below T_{MI} . We argue, however, that the susceptibility data are influenced by FM clustering due to traces of supercooled high-temperature phase and a clue to the true ground state in $\text{Pr}_{0.5}\text{Ca}_{0.5}\text{CoO}_3$

are the published structural data obtained by means of neutron diffraction.^{3,5,7,8}

The structural changes that accompany the M-I transition are summarized in Fig. 1. The Pr-O bond lengths and Co-O-Co angles decrease abruptly on cooling below 100 K, which causes the volume contraction of $\text{Pr}_{0.5}\text{Ca}_{0.5}\text{CoO}_3$. On the other hand, Co-O bond lengths even seem to increase at this temperature, though the change may be insignificant. Based on these facts we suggest that the formal cobalt valency is decreased below T_{MI} from mixed-valency $\text{Co}^{3.5+}$ toward pure Co^{3+} with strong preference for LS state and the praseodymium valency is simultaneously changed from Pr^{3+} toward Pr^{4+} of smaller ionic size. The spin-state transition and formation of an insulating state in $\text{Pr}_{0.5}\text{Ca}_{0.5}\text{CoO}_3$ is thus an analogy of the compositional transition from the ferromagnetic metal $\text{La}_{0.5}\text{Sr}_{0.5}\text{CoO}_3$ to diamagnetic insulator LaCoO_3 .^{2,9} To provide a support for such interpretation and demonstrate the unique role of praseodymium in the M-I transition, we have undertaken comparative *ab initio* electronic-structure calculations for systems $\text{Pr}_{0.5}\text{Ca}_{0.5}\text{CoO}_3$ and $\text{Nd}_{0.5}\text{Ca}_{0.5}\text{CoO}_3$.

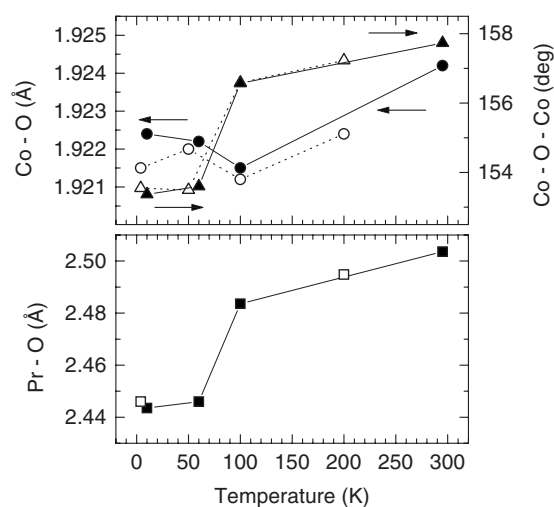


FIG. 1. The temperature dependence of average Co-O (●, 6×) and Pr-O (■, 8×; the four remaining Pr-O distances are considered as nonbonding) bond lengths and Co-O-Co bond angles (▲) in the orthoperovskite structure of $\text{Pr}_{0.5}\text{Ca}_{0.5}\text{CoO}_3$ taken from Ref. 5 (full symbols) and Ref. 8 (open symbols).

TABLE I. Calculated spin moments of $\text{Pr}_{0.5}\text{Ca}_{0.5}\text{CoO}_3$ and $\text{Nd}_{0.5}\text{Ca}_{0.5}\text{CoO}_3$ (in μ_B).

T (K)	$\text{Pr}_{0.5}\text{Ca}_{0.5}\text{CoO}_3$			$\text{Nd}_{0.5}\text{Ca}_{0.5}\text{CoO}_3$		
	Total	Pr($\times 0.5$)	Co($\times 1$)	Total	Nd($\times 0.5$)	Co($\times 1$)
10	0.50	1.39	-0.12	3.00	2.96	1.40
60	0.50	1.39	-0.12	3.00	2.96	1.40
100	2.50	1.97	1.46	3.00	2.96	1.42
300	2.50	1.97	1.48	3.00	2.97	1.47

II. METHOD OF CALCULATION

The calculations were done with the WIEN2K program.¹⁰ This program is based on the density-functional theory (DFT) and uses the full-potential linearized augmented plane wave method with the dual-basis set. The core states were defined as an electronic configuration (Kr, $4d^{10}$) for Pr and Nd, (Ne) for Ca, (Ne, $3s^2$) for Co and as (He) for O atoms. The valence states included $3p$, $3d$, and $4s$ orbitals for Co; $5s$, $5p$, $4f$, $5d$, $6s$, and $6p$ for Pr and Nd. The cell was selected of the same size as the crystallographic $Pnma$ one, containing 4 f.u. $\text{Pr}_{0.5}\text{Ca}_{0.5}\text{CoO}_3$ (20 atoms in cell, 178 valence electrons). The Pr (or Nd) and Ca were distributed in a regular rock-salt manner. All calculations were spin polarized. For the exchange-correlation potential the generalized gradient approximation (GGA) form was adopted.¹¹ The radii of the atomic spheres were taken 2.3 a.u. for Pr, Nd, and Ca, 1.9 a.u. for Co, and 1.6 a.u. for O. To improve the description of Pr $4f$ and Co $3d$ electrons we used the GGA+ U method, which corresponds to local-density approximation (LDA+ U) method described in^{12,13} with the GGA correlation potential instead of LDA. A wide range of U was tested for Pr (1.4–12.2 eV) and for Co (1.4–6.8 eV). The presented results were obtained with $U=6.8$ eV for Pr and Nd, $U=2.7$ eV for Co, and $J=0.95$ eV for both.

Resolving the temperature dependence with the DFT-type method, which basically concerns the ground state, is based on assumption that the changes in electronic structure are driven by the temperature evolution of the crystal structure, and the entropy part of the free energy is marginal. This approach was successfully applied, e.g., for the study of spin transitions in LaCoO_3 .^{14–16} The application of this approach in the present case of $\text{Pr}_{0.5}\text{Ca}_{0.5}\text{CoO}_3$ is even more justifiable since the change in the crystal structure at T_{MI} is abrupt in comparison with a smooth evolution of the LaCoO_3 structure at the spin-state transitions. Namely, the electronic-structure calculations of $\text{Pr}_{0.5}\text{Ca}_{0.5}\text{CoO}_3$ were performed by adopting the crystal structures determined experimentally at temperatures 10, 60, 100, and 300 K in Ref. 5. To investigate the effect of the Ln cation, the structures with identical CoO_6 coordination but with the cell volume contracted by 0.5% were anticipated for $\text{Nd}_{0.5}\text{Ca}_{0.5}\text{CoO}_3$, taking into account that the volume difference between PrCoO_3 and NdCoO_3 is $\sim 1\%$,¹⁷ and the position of Nd atom was optimized during calculation.

III. RESULTS AND DISCUSSION

The local spin moments, calculated for the Pr (or Nd) and Co sites, as well as the total moment per f.u. are collected in

Table I. There is a marked change in the total spin moment in $\text{Pr}_{0.5}\text{Ca}_{0.5}\text{CoO}_3$ from $2.5\mu_B$ at 100 and 300 K to $0.5\mu_B$ at 10 and 60 K, which reproduces well the experimentally observed transition temperature T_{MI} . On the other hand, in the case of $\text{Nd}_{0.5}\text{Ca}_{0.5}\text{CoO}_3$ the magnetic moment per f.u. has a constant value $3\mu_B$ for all temperatures. The results show further that the decrease in the total magnetic moment in $\text{Pr}_{0.5}\text{Ca}_{0.5}\text{CoO}_3$ arises mainly due to a drop of spin moment of Co from ~ 1.5 to ~ 0 but there is also a significant contribution of a decrease in Pr moment from ~ 2 to ~ 1.4 .

The decrease in the praseodymium moment is primarily caused by a change in $4f$ states occupation, which is reproduced in the GGA+ U calculations for all realistic values of the parameter U ,¹⁸ and it is not encountered in the $\text{Nd}_{0.5}\text{Ca}_{0.5}\text{CoO}_3$ system with the Nd^{3+} ions of $4f^3$ electron configuration, see Fig. 2. Simultaneously, the occupation of the hybridized $\text{Co}(3d)\text{-O}(2p)$ orbitals in $\text{Pr}_{0.5}\text{Ca}_{0.5}\text{CoO}_3$ increases with decreasing temperature. These findings are consistent with our idea that the cobalt spin-state transition in $\text{Pr}_{0.5}\text{Ca}_{0.5}\text{CoO}_3$ at $T_{\text{MI}}=90$ K is conditioned by a transfer of electron holes from cobalt to the praseodymium sites.

The details of the phase transition in $\text{Pr}_{0.5}\text{Ca}_{0.5}\text{CoO}_3$ in distinction to conventional situation in $\text{Nd}_{0.5}\text{Ca}_{0.5}\text{CoO}_3$ become more apparent by inspection of the density of states (DOS), displayed in Fig. 3. The $\text{Co}(3d)$ and $\text{O}(2p)$ bands of $\text{Pr}_{0.5}\text{Ca}_{0.5}\text{CoO}_3$ at 300 K [Fig. 3(b)] are broad, indicating strong hybridization between these atoms. Finite DOS at E_F in majority spin is contributed by the σ states formed by e_g orbitals, while the minority spin bands, contributed mainly by t_{2g} orbitals, show a gap. Certain degree of hybridization is evident also for the occupied Pr($4f$) states, which are broad and only ~ 0.5 eV below Fermi level. The character of $\text{Co}(3d)\text{-O}(2p)$ band of $\text{Nd}_{0.5}\text{Ca}_{0.5}\text{CoO}_3$ [Fig. 3(d)] is very similar to that of $\text{Pr}_{0.5}\text{Ca}_{0.5}\text{CoO}_3$, but significant difference is in the character of the occupied Nd($4f$) band, which is lo-

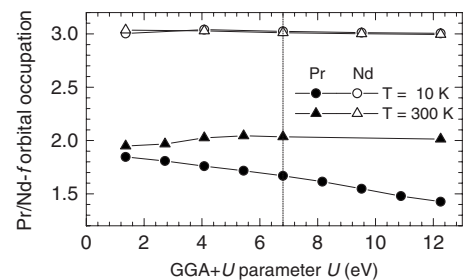


FIG. 2. Dependence of Pr (full symbols) and Nd (open symbols) f -orbital occupation on parameter U for 300 K (▲) and 10 K (●). The value of U used for calculation is indicated.

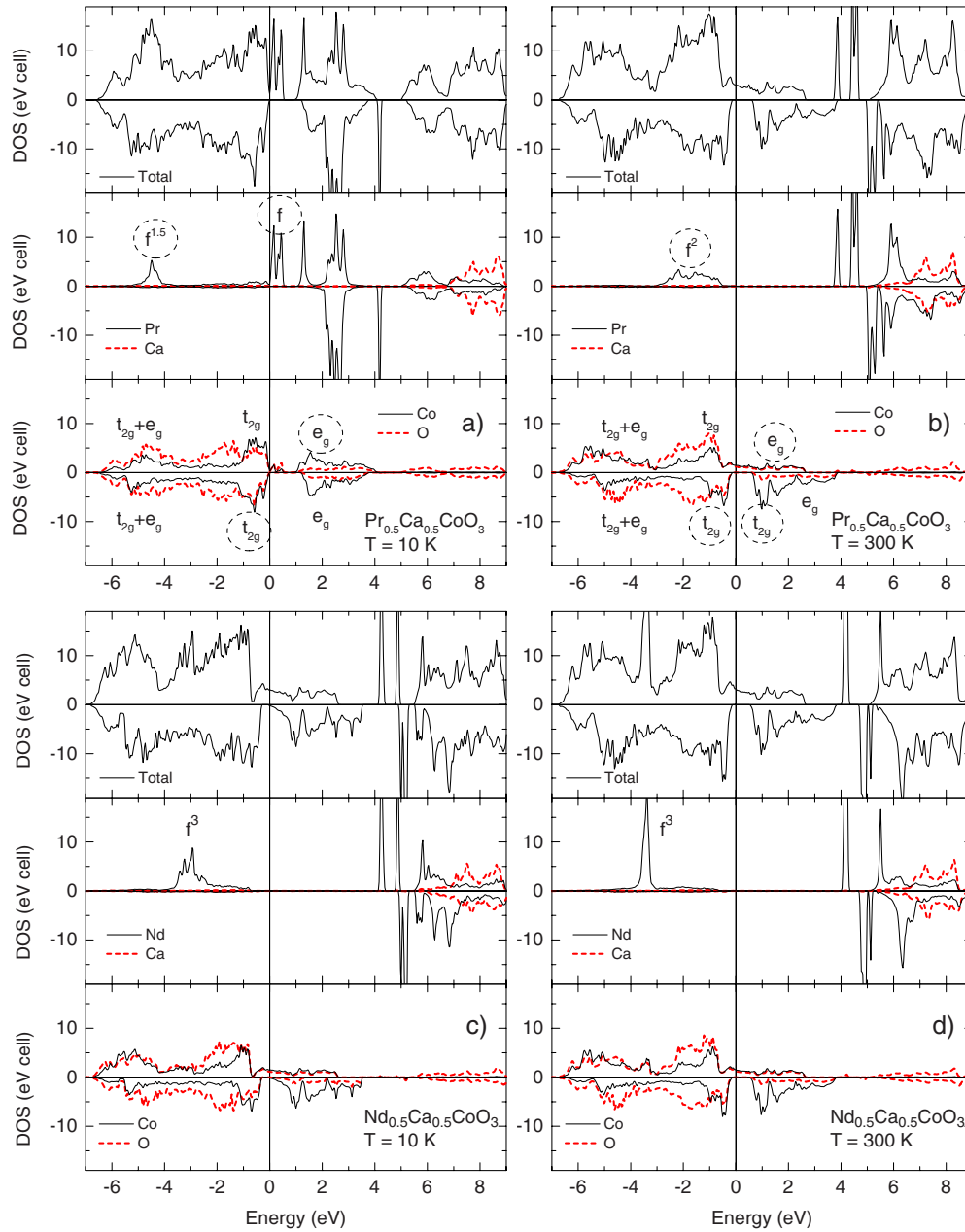


FIG. 3. (Color online) DOS for [(a) and (b)] $\text{Pr}_{0.5}\text{Ca}_{0.5}\text{CoO}_3$ and [(c) and (d)] $\text{Nd}_{0.5}\text{Ca}_{0.5}\text{CoO}_3$ at [(a) and (c)] 10 K and [(b) and (d)] 300 K. The partial DOS most affected by the M-I transition in $\text{Pr}_{0.5}\text{Ca}_{0.5}\text{CoO}_3$ are marked by a dashed circle.

cated deeply below Fermi level and is narrow since its overlap with oxygen bands is obviously small. As regards the empty Pr and Nd bands, there are both about 4 eV above E_F .

The different character of the occupied Pr and Nd f bands in $\text{Pr}_{0.5}\text{Ca}_{0.5}\text{CoO}_3$ and $\text{Nd}_{0.5}\text{Ca}_{0.5}\text{CoO}_3$ at 300 K is crucial for the evolution of the respective DOS at lower temperature. The occupied Nd($4f$) band at 10 K [Fig. 3(c)] becomes broader due to the shortening of Nd-O bonds but it still completely remains below the Fermi level thus keeping its occupation f^3 . The character of Co($3d$)-O($2p$) band remains practically unchanged. On the other hand, the occupied Pr($4f$) band at 10 K splits and a part of originally occupied states shifts above Fermi level [Fig. 3(a)]. The electrons from Pr($4f$) band move to the hybridized Co($3d$)-O($2p$) band. A gap opens in Co-O band in both the majority and minority

spins. The replacement of broad Co-O band by a narrow Pr band around and above Fermi level explains an increase in resistivity observed in the experiment.

The magnitude of the Co($3d$)-O($2p$) band gap at $T = 10$ K depends on the chosen value of the parameter U for the corresponding orbital. In our case the gap is ~ 0.9 eV for $U = 2.7$ eV and it opens wider with increasing U while the half-metallic character at $T = 300$ K is preserved. There is no unique value for U but the chosen value is close to the lower limit of U for Co in oxides (for discussion see, e.g., Ref. 19).

To estimate quantitatively what is the actual charge transfer is a more complex task in the GGA+ U calculation. Unlike the spin density which is ~ 97 – 98% confined in atomic spheres, the charge density of valence electrons is distributed over the whole lattice. The number of electrons allocated to

TABLE II. Charges at atom sites for $\text{Pr}_{0.5}\text{Ca}_{0.5}\text{CoO}_3$ and $\text{Nd}_{0.5}\text{Ca}_{0.5}\text{CoO}_3$ calculated by AIM method.

T (K)	Pr($\times 0.5$)	Ca($\times 0.5$)	Co($\times 1$)	O($\times 3$)
10	2.29	1.56	1.47	-1.13
60	2.29	1.56	1.48	-1.13
100	2.09	1.57	1.52	-1.12
300	2.10	1.57	1.52	-1.12

T (K)	Nd($\times 0.5$)	Ca($\times 0.5$)	Co($\times 1$)	O($\times 3$)
10	2.08	1.56	1.52	-1.11
300	2.10	1.57	1.52	-1.12

individual cations, and consequently the charge of the cation, thus depends to some extent on the radius of chosen atomic spheres. A more suitable method to quantify the atomic charges is the atoms-in-molecule (AIM) concept of Bader.²⁰ In this approach the unit cell is divided into regions by surfaces that run through the minima in the charge density. A region enclosed by such boundary surfaces and containing one nucleus is referred to as a Bader region. By integrating the electronic density within the Bader region the total excess charge on a given site can be calculated. The advantage of this method is that the analysis is based solely on the charge density so it is independent on the basis set and atomic spheres used.

The resulting atomic charges for $\text{Pr}_{0.5}\text{Ca}_{0.5}\text{CoO}_3$ and $\text{Nd}_{0.5}\text{Ca}_{0.5}\text{CoO}_3$ are displayed in Table II. The calculated charges differ from the ideal ones due to hybridization between cations and oxygen. The ratio of the AIM and ideal charge may be regarded as the degree of hybridization. At 300 K this ratio is similar both for $\text{Pr}_{0.5}\text{Ca}_{0.5}\text{CoO}_3$ and $\text{Nd}_{0.5}\text{Ca}_{0.5}\text{CoO}_3$, namely, 0.79 for Ca^{2+} , 0.70 for Pr^{3+} and Nd^{3+} , and 0.44 for $\text{Co}^{3.5+}$.

The temperature variation in the atom charges in $\text{Nd}_{0.5}\text{Ca}_{0.5}\text{CoO}_3$ is very small and can be associated with

slightly increasing hybridization due to the shortening distances between atoms with decreasing temperature. In the case of $\text{Pr}_{0.5}\text{Ca}_{0.5}\text{CoO}_3$ the charge of Pr significantly increases between 100 and 60 K from 2.09 to 2.29. An opposite and smaller change is observed for Co, whose charge is decreasing from 1.52 to 1.48. The oxygen charge variation is only subtle, it slightly increases with decreasing temperature contrary to the trend in $\text{Nd}_{0.5}\text{Ca}_{0.5}\text{CoO}_3$. When the neodymium system is taken as reference, it is evident that the shift of Pr and Co charges cannot be explained by a change in a degree of hybridization but it must be attributed to the charge transfer between Pr and Co.

IV. CONCLUSION

In summary, our spin-polarized GGA+ U calculations evidence that the metal-insulator transition in $\text{Pr}_{0.5}\text{Ca}_{0.5}\text{CoO}_3$ is associated with an electron drain from the praseodymium positions and formation of a nonmagnetic state on the cobalt positions. These circumstances are in essential agreement with an ionic scenario presuming a valence shift from Pr^{3+} to Pr^{4+} and from paramagnetic $\text{Co}^{3.5+}$ ($t_{2g}^3\sigma^{0.5}$) to diamagnetic LS Co^{3+} (t_{2g}^6), though the total charges localized on the respective sites change less than the ideal model supposes due to the strongly covalent character of the system. Nevertheless, the simple ionic picture remains relevant for understanding other properties of $\text{Pr}_{0.5}\text{Ca}_{0.5}\text{CoO}_3$ such as the temperature behavior of paramagnetic susceptibility. It is important to note, that the structural changes as observed in $\text{Pr}_{0.5}\text{Ca}_{0.5}\text{CoO}_3$, in particular, the contraction of the rare-earth—oxygen bonds and modified tilt of the CoO_6 octahedra, are not themselves sufficient condition for the occurrence of the phase transition, as evidenced by the comparative calculation with Nd instead of Pr, but the influence of the charge transfer between Pr and Co cations is essential.

ACKNOWLEDGMENT

This work was supported under Project No. 202/09/0421 of the Grant Agency of the Czech Republic.

¹T. Fujita, S. Kawabata, M. Sato, N. Kurita, M. Hedo, and Y. Uwatoko, *J. Phys. Soc. Jpn.* **74**, 2294 (2005).

²K. Knížek, Z. Jiráček, J. Hejtmanek, and P. Novák, *J. Magn. Magn. Mater.* **322**, 1221 (2010).

³S. Tsubouchi, T. Kyômen, M. Itoh, P. Ganguly, M. Oguni, Y. Shimojo, Y. Morii, and Y. Ishii, *Phys. Rev. B* **66**, 052418 (2002).

⁴S. Tsubouchi, T. Kyômen, M. Itoh, and M. Oguni, *Phys. Rev. B* **69**, 144406 (2004).

⁵T. Fujita *et al.*, *J. Phys. Soc. Jpn.* **73**, 1987 (2004).

⁶T. Naito, H. Sasaki, and H. Fujishiro, *J. Phys. Soc. Jpn.* **79**, 034710 (2010).

⁷A. V. Chichev, M. Dlouhá, S. Vratislav, J. Hejtmanek, Z. Jiráček, K. Knížek, and M. Maryško, *Z. Kristallogr. Suppl.* **26**, 435

(2007).

⁸P. Tong, Y. Wu, B. Kim, D. Kwon, J. M. S. Park, and B. G. Kim, *J. Phys. Soc. Jpn.* **78**, 034702 (2009).

⁹J. Wu and C. Leighton, *Phys. Rev. B* **67**, 174408 (2003).

¹⁰P. Blaha, K. Schwarz, G. K. H. Madsen, D. Kvasnicka, and J. Luitz, *WIEN2K, An Augmented Plane Wave Plus Local Orbitals Program for Calculating Crystal Properties* (Technische Universität, Wien, 2001).

¹¹J. P. Perdew, K. Burke, and M. Ernzerhof, *Phys. Rev. Lett.* **77**, 3865 (1996).

¹²V. I. Anisimov, I. V. Solovyev, M. A. Korotin, M. T. Czyzyk, and G. A. Sawatzky, *Phys. Rev. B* **48**, 16929 (1993).

¹³A. I. Liechtenstein, V. I. Anisimov, and J. Zaanen, *Phys. Rev. B* **52**, R5467 (1995).

- ¹⁴M. A. Korotin, S. Yu. Ezhov, I. V. Solovyev, V. I. Anisimov, D. I. Khomskii, and G. A. Sawatzky, *Phys. Rev. B* **54**, 5309 (1996).
- ¹⁵K. Knížek, Z. Jiráček, J. Hejtmánek, and P. Novák, *J. Phys.: Condens. Matter* **18**, 3285 (2006).
- ¹⁶K. Knížek, Z. Jiráček, J. Hejtmánek, P. Novák, and W. Ku, *Phys. Rev. B* **79**, 014430 (2009).
- ¹⁷K. Knížek, J. Hejtmánek, Z. Jiráček, P. Tomeš, P. Henry, and G. André, *Phys. Rev. B* **79**, 134103 (2009).
- ¹⁸P. Larson, W. R. L. Lambrecht, A. Chantis, and M. van Schilf-gaarde, *Phys. Rev. B* **75**, 045114 (2007).
- ¹⁹F. Tran, P. Blaha, K. Schwarz, and P. Novák, *Phys. Rev. B* **74**, 155108 (2006).
- ²⁰R. F. W. Bader, *Atoms in Molecules: A Quantum Theory* (Oxford University Press, Oxford, 1990).